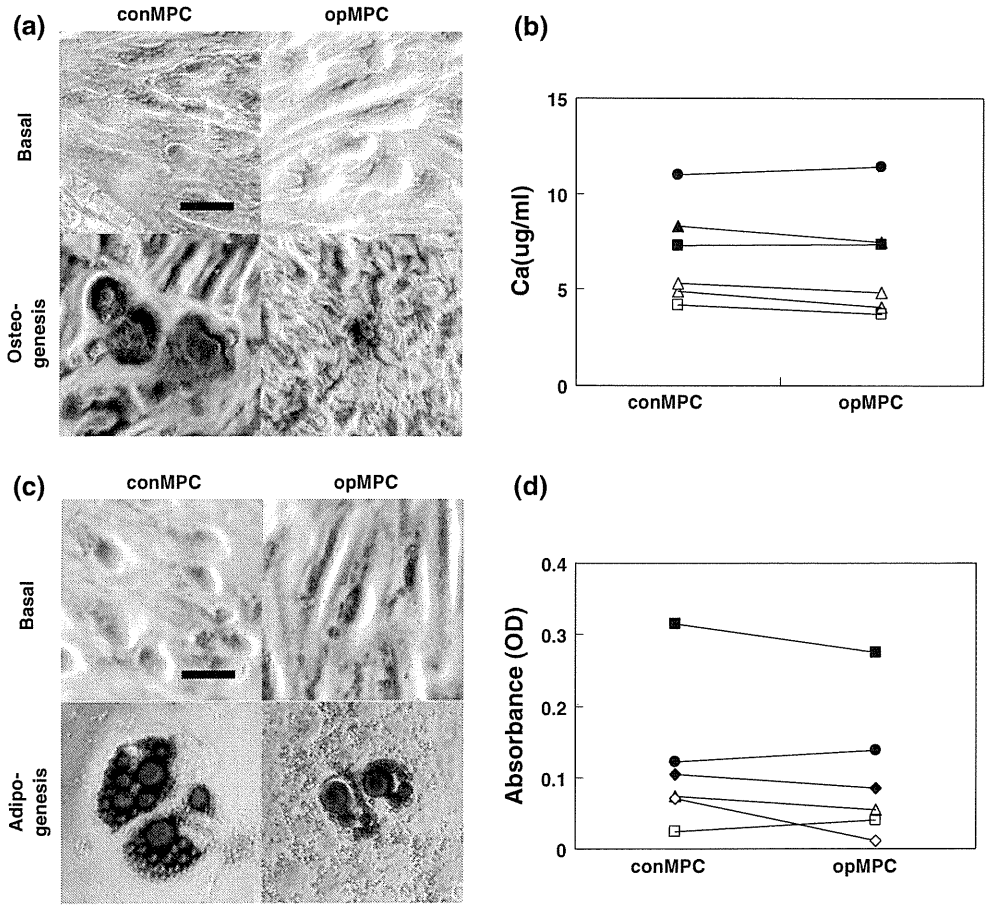

Fig. 3 Comparison of the osteogenic and adipogenic potential between opMPC and conMPC. **a** Photomicrographs of opMPC and conMPC cultured in basic culture medium (control) or osteogenic medium (osteogenesis) stained with alizarin red. *Bar* 25 μm. **b** Calcium content of cells cultured in osteogenic medium. **c** Photomicrographs of opMPC and conMPC cultured in basic culture medium (control) or adipogenic induction medium (adipogenesis) stained with oil red O. *Bar* 25 μm. **d** Elution of Oil Red O from opMPC and conMPC following exposure to adipogenic medium. *Filled triangle, filled square, filled circle, open diamond, open square, open triangle*: sheep 1–6. No significant differences were detected

biomarkers between opMPCs and conMPCs at passage 2 were compared. Quantitative RT-PCR revealed that mRNA levels for IL-1β, MMP-3, and MMP-13 normalized to 18S in opMPCs remained somewhat higher than those in conMPCs; however, significant differences were not detected due to large animal-to-animal variation (Fig. 4a–c). Trends for higher mRNA levels for MMP-13 (Fig. 4c) in opMPCs compared to the corresponding conMPCs were observed in all animals, while such trends were observed for IL-1β (Fig. 4a) and MMP-3 (Fig. 4b) in cells from five of six animals.

Effect of exogenous IL-1β on the chondrogenic potential of SM-derived normal cells

To examine the potential involvement of inflammatory mediators in the observed inhibition of chondrogenesis by cells from surgically affected joints, 0–100 nM of IL-1β were added during the chondrogenic differentiation of MPCs from normal sheep SM. The cross-sectional area of normal SM-MPC pellets cultured in the chondrogenic medium with >1 nM IL-1β were significantly reduced compared to those cultured in chondrogenic medium without IL-1β (Fig. 5).

Discussion

In this study, it has been demonstrated that surgical intervention to the ovine knee joint results in increases in the volume of SF in the joints, as well as elevations in mRNA levels for some catabolic biomarkers in the corresponding SM by 2 weeks post-surgery. In addition, and critical to the effectiveness of endogenous MPCs, it was demonstrated that cells from SM exposed to surgery-associated inflammation maintained over-expression of inflammatory

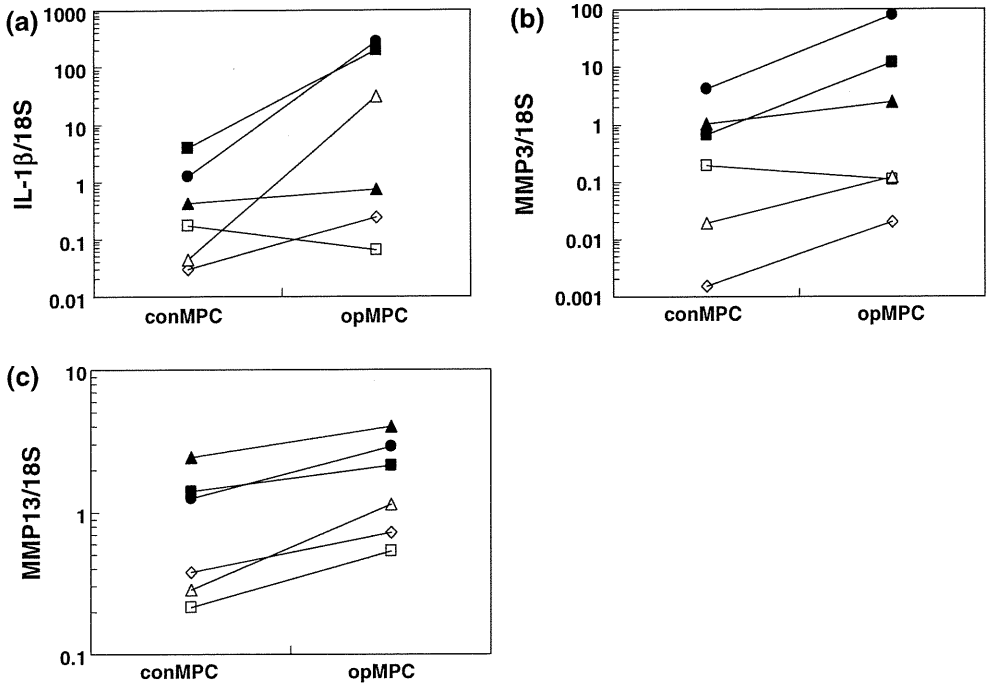

Fig. 4 mRNA levels for inflammatory mediators and MMPs in the SM after surgery. Quantification of the results of RT-qPCR analysis inflammatory mediators and MMPs including IL-1β (**a**), MMP-3 (**b**), and MMP-13 (**c**) normalized to 18S in SM-MPCs derived from the operated (*opMPC*) and contralateral (*conMPC*) knees of the sheep at 2 weeks after ACL reconstruction surgery. *Filled triangle, filled square, filled circle, open diamond, open square, open triangle*: sheep 1–6

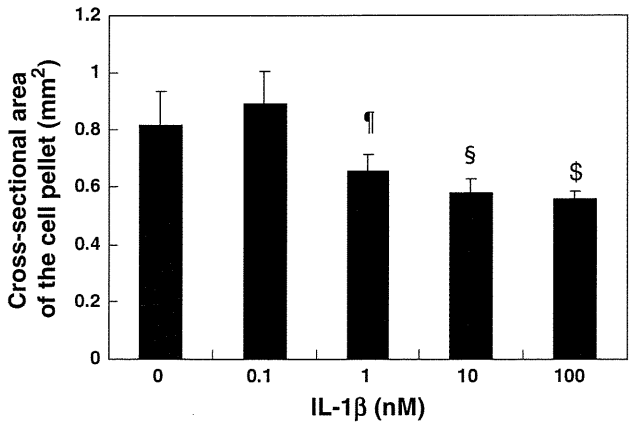

Fig. 5 Chondrogenic potential under IL-1β stimulation: ratio of sectional area from 2D images of MPCs from normal sheep SM cultured in chondrogenic induction medium with 0–100 nM IL-1β. $^{¶}p = 0.01$, $^{§}p < 0.001$, $^{\$}p < 0.001$ compared to MPC pellets cultured in chondrogenic induction medium without IL-1β. $N = 4$

biomarkers and uniquely exhibited lower chondrogenic differentiation capacity (~70% of control values) compared to cells from the contralateral knee. It was also shown that in-vitro exposure to 1–100 nM of exogenous IL-1β also led to diminished chondrogenic differentiation capacity of SM-MPCs from normal sheep.

Inflammatory mediators including IL-1β and TNFα have been reported to decrease the mRNA levels for chondrogenic markers including Col2A1 and aggrecan during chondrogenesis of BM-MSCs and SM-MSCs, respectively, under the influences of BMP2 in a dose-dependent manner [35, 36]. These inflammatory mediators were also reported to inhibit chondrogenesis induced by TGFα [37], as well as osteogenesis [38] by human BM-MSCs. The present results and the reports from other laboratories suggest that inflammatory cytokines are potentially involved in the suppression of the chondrogenic capacity of cells exposed to inflammation, and that this suppressive effect on chondrogenic capacity by MPCs exposed to inflammation may also contribute to the unstable balance between degradative and biosynthetic events within the joints, an imbalance which could ultimately contribute to OA development and progression.

In contrast to other reports with human BM-MSCs [38], we did not detect differences in osteogenic and adipogenic potential between cells isolated from the SM from operated knees compared to those from contralateral knees. We speculate that part of this discrepancy may be based on the relatively low osteogenic/adipogenic potential of the cells derived from the SM compared to their chondrogenic potential, or perhaps species or tissue origin differences.

Metalloproteinases are reported to play central roles in tissue repair and remodeling of connective tissues in response to injury, as well as being involved in destructive disease processes including OA [39]. They are sub-grouped

into collagenases (MMP-1, MMP-8, MMP-13, and MMP-18), gelatinases (MMP-2 and MMP-9), stromelysins (MMP-3, MMP-10, and MMP-11), matrilysins, membrane-type (MT)-MMPs, and others [40]. In the present study, mRNA levels for MMP-3 and MMP-13 in SM tissue from operated knees were significantly higher than those from contralateral knees, but the differences in mRNA levels for MMP-2 were trends only. MMPs are synthesized as pre-proenzymes and processed by tissue and plasma proteinase including other active MMPs to become active MMPs that can digest a number of ECM molecules including collagens and aggrecans [40]. Furthermore, several of the differences in mRNA levels for MMPs between conMPC and opMPC were also only trends; however, GAG measurement in chondrogenic cell pellets showed significant differences between conMPC and opMPC cultures.

With regard to the effect of exogenous IL-1β on chondrogenic differentiation of normal SM-MPCs, a number of interesting points are raised by the data. First, exposure to IL-1β led to decreases in chondrogenesis to $\sim$70% of control values. This level of decline was similar to that detected between the opMPC and conMPC cultures. However, it remains to be determined whether IL-1β is the primary endogenous effector cytokine in vivo. Secondly, the inhibition of chondrogenesis following exposure to the exogenous IL-1β appeared to be nearly maximal with 10 nM of IL-1β and no further declines were detected when concentrations were increased to 100 nM. Thus, it would appear that only a subset of SM-MPCs are susceptible to the inhibitory influences of this cytokine in vivo, and it is curious that there is such correlation between the levels of inhibition of chondrogenesis in the opMPC compared to the conMPC, and the in-vitro IL-1β studies. At a minimum, the findings imply there are multiple subsets of MSCs/MPCs in the SM from normal sheep, some being responsive to IL-1β and others resistant to the biological effects of the cytokine. Whether such response patterns relate to expression of IL-1 receptors by a subset of MPCs is the subject of current studies.

While the results presented clearly show how inflammation in the surgically altered knee joint leads to decreased potential for synovial membrane MSCs to differentiate towards the chondrogenic phenotype, there are some limitations to the studies presented. First, the number of animals assessed is not large. However, we have used a large animal model and it is difficult to use a substantial number due to cost and ability to house and train large numbers of animals. This limitation is off-set by using a large animal with knee components not unlike those of the human. Second, we are able to obtain as much synovial fluid as possible, but have no way of determining whether we obtained all of it when trying to quantify volumes. However, the method used was reproducible in our hands. Thirdly, we obtained synovial membranes from reproducible sites, but we do not know if there are site-specific differences, and whether the altered proteinase levels contributed to the selective release of subsets of MSCs from the synovium which could have influenced the findings. Fourthly, we measured mRNA, but not corresponding protein levels so cannot with certainty say the mRNA levels led to alterations in protein levels for specific molecules. Moreover, an additional limitation of this study is that only one point of the acute post-surgery stage was investigated. It has been reported that IL-6 and TNFα levels in SF decline with time after ACL injury, but remain considerably elevated chronically (3 months) [13]. It remains unclear whether the prolonged exposure of the MPCs to chronic inflammation would further compromise mRNA levels for relevant molecules and chondrogenic capacities. Further investigation will be needed to clarify the potential influence of duration of exposure to inflammation on the function of the cells and whether they recover function in vitro with increasing cell passage number. Such issues are the subject of current studies. Finally, we only assessed mRNA levels for a few molecules, and future studies should expand the repertoire of molecules assessed. In spite of these limitations, the results presented are novel and indicate that the joint environment can influence the phenotype of the synovial membrane-associated MSCs.

We conclude that cells from tissue exposed to post-surgery inflammation continue to over-express inflammatory biomarkers that can affect the chondrogenic potential of MPCs, suggesting that MPCs from injured joints are compromised and retain the compromised phenotype regarding their endogenous repair potential.

Acknowledgments We thank Craig Sutherland and Carol Reno for technical assistance with the sheep surgery and the RT-qPCR analysis, respectively. The authors also thank Dr. Yamini Achari for editorial assistance. This research was supported by the Uehara Memorial Foundation, an Osteoarthritis Team Grant from the Alberta Heritage Foundation for Medical Research, a CHIR grant to C.B.F. and N.G.S. focussed on the sheep model, and the CIHR Institute for the Gender and Health. D.A.H. is the Calgary Foundation–Grace Glaum Professor and C.B.F. is the McCaig Professor. W.A. is a fellow of the UMF and AHFMR.

Conflict of interest The authors report no conflict of interest. The authors alone are responsible for the content and writing of the paper.

References

1. Pittenger MF, Mackay AM, Beck SC, Jaiswal RK, Douglas R, Mosca JD, et al. Multi-lineage potential of adult human mesenchymal stem cells. Science. 1999;284:143–7.
2. Jankowski RJ, Deasy BM, Huard J. Muscle-derived stem cells. Gene Ther. 2002;9:642–7.
3. De Bari C, Dell'Accio F, Tylzanowski P, Luyten FP. Multipotent mesenchymal stem cells from adult human synovial membrane. Arthritis Rheum. 2001;44:1928–42.

4. Wickham MQ, Erickson GR, Gimble JM, Vail TP, Guilak F. Multipotent stromal cells derived from the infrapatellar fat pad of the knee. Clin Orthop. 2003;412:196–212.
5. Lee OK, Kuo TK, Chen WM, Lee KD, Hsieh SL, Chen TH. Isolation of multipotent mesenchymal stem cells from umbilical cord blood. Blood. 2003;103:1669–75.
6. Miao Z, Jin J, Chen L, Zhu J, Huang W, Zhao J, et al. Isolation of mesenchymal stem cells from human placenta: comparison with human bone marrow mesenchymal stem cells. Cell Biol Int. 2006;30:681–7.
7. Sakaguchi Y, Sekiya I, Yagishita K, Muneta T. Comparison of human stem cells derived from various mesenchymal tissues: superiority of synovium as a cell source. Arthritis Rheum. 2005;52:2521–9.
8. Ando W, Tateishi K, Hart DA, Katakai D, Tanaka Y, Nakata K, et al. Cartilage repair using in vitro generated scaffold-free tissue engineered construct derived from porcine synovial mesenchymal stem cells. Biomaterials. 2007;28:5462–70.
9. Mor A, Abramson SB, Pillinger MH. The fibroblast-like synovial cell in rheumatoid arthritis: a key player in inflammation and joint destruction. Clin Immunol. 2005;115(2):118–28.
10. Jones EA, English A, Henshaw K, Kinsey SE, Markham AF. Enumeration and phenotypic characterization of synovial fluid multipotential mesenchymal progenitor cells in inflammatory and degenerative arthritis. Arthritis Rheum. 2004;50:817–27.
11. Harvanová D, Tóthová T, Sarišský M, Amrichová J, Rosocha J. Isolation and characterization of synovial mesenchymal stem cells. Folia Biol (Praha). 2011;57(3):119–24.
12. Fernandes JC, Martel-Pelletier J, Pelletier JP. The role of cytokines in osteoarthritis pathophysiology. Biorheology. 2002;39:237–46.
13. Cameron M, Buchgraber A, Passler H, Vogt M, Thonar E, Fu F, et al. The natural history of the anterior cruciate ligament-deficient knee. Changes in synovial fluid cytokine and keratan sulfate concentrations. Am J Sports Med. 1997;25:751–4.
14. Irie K, Uchiyama E, Iwaso H. Intraarticular inflammatory cytokines in acute anterior cruciate ligament injured knee. Knee. 2003;10:93–6.
15. Higuchi H, Shirakura K, Kimura M, Terauchi M, Shinozaki T, Watanabe H, et al. Changes in biochemical parameters after anterior cruciate ligament injury. Int Orthop. 2006;30:43–7.
16. Marks PH, Donaldson ML. Inflammatory cytokine profiles associated with chondral damage in the anterior cruciate ligament-deficient knee. Arthroscopy. 2005;21:1342–7.
17. Tung JT, Fenton JI, Arnold C, Alexander L, Yuzbasiyan-Gurkan V, Venta PJ, et al. Recombinant equine interleukin-1beta induces putative mediators of articular cartilage degradation in equine chondrocytes. Can J Vet Res. 2002;66:19–25.
18. Jasser MZ, Mitchell PG, Cheung HS. Induction of stromelysin-1 and collagenase synthesis in fibrochondrocytes by tumor necrosis factor-alpha. Matrix Biol. 1994;14:241–9.
19. Murphy JM, Dixon K, Beck S, Fabian D, Feldman A, Barry F. Reduced chondrogenic and adipogenic activity of mesenchymal stem cells from patients with advanced osteoarthritis. Arthritis Rheum. 2002;46:704–13.
20. Alsalameh S, Amin R, Gemba T, Lotz M. Identification of mesenchymal progenitor cells in normal and osteoarthritic human articular cartilage. Arthritis Rheum. 2004;50:1522–32.
21. Dudics V, Kunstár A, Kovács J, Lakatos T, Géher P, Gömör B, et al. Chondrogenic potential of mesenchymal stem cells from patients with rheumatoid arthritis and osteoarthritis: measurements in a microculture system. Cells Tissues Organs. 2009;89:307–16.
22. Scharstuhl A, Mutsaers HA, Pennings SW, Szarek WA, Russel FG, Wagener FA. Chondrogenic potential of human adult mesenchymal stem cells is independent of age or osteoarthritis etiology. Stem Cells. 2007;25:3244–51.
23. Frank CB, Jackson DW. The science of reconstruction of the anterior cruciate ligament. J Bone Joint Surg Am. 1997;79:1556–76.
24. Fleming BC, Hulstyn MJ, Oksendahl HL, Fadale PD. Ligament injury reconstruction and osteoarthritis. Curr Opin Orthop. 2005;16:354–62.
25. Heard BJ, Achari Y, Chung M, Shrive NG, Frank CB. Early joint tissue changes are highly correlated with a set of inflammatory and degradative synovial biomarkers after ACL autograft and its sham surgery in an ovine model. J Orthop Res. 2011;29(8):1185–92.
26. Kuh SU, Zhu Y, Li J, Tsai KJ, Fei Q, Hutton WC, et al. Can TGF-beta1 and rhBMP-2 act in synergy to transform bone marrow stem cells to discogenic-type cells? Acta Neurochir (Wien). 2008;150:1073–9.
27. Tateishi K, Higuchi C, Ando W, Nakata K, Hashimoto J, Hart DA, et al. The immunosuppressant FK506 promotes development of the chondrogenic phenotype in human synovial stromal cells via modulation of the Smad signaling pathway. Osteoarthr Cartil. 2007;15:709–18.
28. Magari K, Nishigaki F, Sasakawa T, Ogawa T, Miyata S, Ohkubo Y, et al. Anti-arthritic properties of FK506 on collagen-induced arthritis in rats. Inflamm Res. 2003;52:524–9.
29. Reno C, Marchuk L, Sciore P, Frank CB, Hart DA. Rapid isolation of total RNA from small samples of hypocellular, dense connective tissues. Biotechniques. 1997;22:1082–6.
30. Nakajima I, Muroya S, Chikuni K. Growth arrest by octanoate is required for porcine preadipocyte differentiation. Biochem Biophys Res Commun. 2003;309:702–8.
31. Hong L, Colpan A, Peptan IA. Modulations of 17-beta estradiol on osteogenic and adipogenic differentiations of human mesenchymal stem cells. Tissue Eng. 2006;12:2747–53.
32. Hellio Le Graverand MP, Reno C, Hart DA. Heterogenous response of knee cartilage to pregnancy in the rabbit: assessment of specific mRNA levels. Osteoarthr Cartil. 2000;8:53–62.
33. Lu T, Achari Y, Rattner JB, Hart DA. Evidence that estrogen receptor beta enhances MMP-13 promoter activity in HIG-82 cells and that this enhancement can be influenced by ligands and involves specific promoter sites. Biochem Cell Biol. 2007;85:326–36.
34. Zou L, Zou X, Chen L, Li H, Mygind T, Kassem M, et al. Multilineage differentiation of porcine bone marrow stromal cells associated with specific gene expression pattern. J Orthop Res. 2008;26:56–64.
35. Majumdar MK, Wang E, Morris EA. BMP-2 and BMP-9 promotes chondrogenic differentiation of human multipotential mesenchymal cells and overcomes the inhibitory effect of IL-1. J Cell Physiol. 2001;189:275–84.
36. Okuma-Yoshioka C, Seto H, Kadono Y, Hikita A, Oshima Y, Kurosawa H, et al. Tumor necrosis factor-alpha inhibits chondrogenic differentiation of synovial fibroblasts through p38 mitogen activating protein kinase pathways. Mod Rheumatol. 2008;18:366–78.
37. Wehling N, Palmer GD, Pilapil C, Liu F, Wells JW, Müller PE, et al. Interleukin-1beta and tumor necrosis factor alpha inhibit chondrogenesis by human mesenchymal stem cells through NF-kappaB-dependent pathways. Arthritis Rheum. 2009;60:801–12.
38. Lacey DC, Simmons PJ, Graves SE, Hamilton JA. Proinflammatory cytokines inhibit osteogenic differentiation from stem cells: implications for bone repair during inflammation. Osteoarthr Cartil. 2009;17:735–42.
39. Murphy G, Nagase H. Reappraising metalloproteinases in rheumatoid arthritis and osteoarthritis: destruction or repair? Nat Clin Pract Rheumatol. 2008;4:128–35.
40. Nagase H, Visse R, Murphy G. Structure and function of matrix metalloproteinases and TIMPs. Cardiovasc Res. 2006;69:562–73.

Morphological Observations of Mesenchymal Stem Cell Adhesion to a Nano-Periodic Structured Titanium Surface Patterned Using Femtosecond Laser Processing

Kei Oya[1], Shun Aoki[2], Kazunori Shimomura[3], Norihiko Sugita[3], Kenji Suzuki[4], Norimasa Nakamura[3], and Hiromichi Fujie[2,1]*

[1] *Research Institute for Science and Technology, Kogakuin University, 2665-1 Nakano-machi, Hachioji-city, Tokyo 192-0015, Japan*

[2] *Graduate School of System Design, Tokyo Metropolitan University, 6-6 Asahigaoka, Hino-city, Tokyo 191-0065, Japan*

[3] *Graduate School of Medicine, Osaka University, 2-2 Yamadaoka, Suita-city, Osaka 565-0871, Japan*

[4] *Department of Mechanical Systems Engineering, Kogakuin University, 2665-1 Nakano-machi, Hachioji-city, Tokyo 192-0015, Japan*

Abstract:

It is known that the adhesive and anisotropic properties of cell-derived biomaterials are affected by micro- or nano-scale structures processed on culture surface. In the present study, the femtosecond laser processing technique was used to scan a laser beam at an intensity around ablation threshold level on a titanium surface for nano-scale processing. Microscopic observation revealed that the processed titanium exhibited a periodic-patterned groove structure at the surface; the width and depth of the groove were 292 ± 50 nm and 99 ±

31 nm, respectively, and the periodic pitch of the groove was 501 ± 100 nm. Human synovium-derived mesenchymal stem cells were cultured on the surface at the cell density of 3.0×10^3 cells/cm^2 after 4-time cell passage. For comparison, the cells were also cultured on a non-processed titanium surface at the condition identical to the processed surface. Results revealed that the duration for cell attachment to the surface was dramatically reduced on the processed titanium as compared with the non-processed titanium. Moreover, on the processed titanium, cell extension area was significantly increased while cell orientation was aligned along the direction of the periodic grooves. These results suggest that the femtosecond laser processing improves the adhesive and anisotropic properties of cells by producing the periodic nano-scale structure on titanium culture surfaces.

* Corresponding author. Phone/fax: +81 42 585 8628

E-mail address: fujie@sd.tmu.ac.jp

1. Introduction

Titanium and its alloys are widely used as implant biomaterials because they have various excellent properties as follows: [1] high-specific strength and good corrosion resistance, [2] mechanically compatible Young's modulus lower than those of stainless steels and cobalt-chromium alloys, and [3] no cytotoxicity to a living body. Various biofunctions such as adhesiveness and anisotropy are required for biomaterials and medical devices depending on body parts to which they are applied. The most simple and effective method for providing metals with those biofunctions may be the use of surface treatment and modification techniques. Numerous research groups have improved the biocompatibility of biomaterials using the techniques and some of them have already been commercialized.

A biofunction required for most of biomaterials is adequate cell adhesiveness. It has been demonstrated that a material surface processed in micro- or nano-level promotes the cellular adhesiveness.[1-3] Widely spread and the most convenient method of materials is etching process; chemical etching[4,5] or electrochemical etching[6,7] so called wet etching, and ion beam processing[8,9] or reactive ion etching[10,11] so called dry etching. A lot of substrates can be created at a short time with low-cost in wet etching, while a processing with high aspect ratio is possible with a variety of choices for patterns and material in dry etching. However, in wet and dry etching, it was problematic that chemical components remained on the material surfaces are harmful to cells and cell-derived biomaterials. On the other hand, laser processing is a clean technique for surface processing and modification through physical phenomena such as melting or evaporating. Therefore, it is free from chemical contamination on a laser-processed surface. Laser beam processing is categorized into thermal processing and ablation processing. Although the former can be applied to many objects, processed surface may be oxidized by heating. As a result, the composition and

thickness of surface oxide layer are changed in case of metal. The latter, laser ablation, can solve the above-described problem and can be usually performed by the use of femtosecond laser processing system. The laser system can irradiate a fine ranged laser beam with a strong intensity because the laser pulse is compressed to a femtosecond level. Therefore, the heat damages are mostly suppressed, since the laser irradiation breaks up before energy transfer from electrons to lattice ions and the heat-affected zone is quite small.[12] Previous studies reported that a nano-sized grating (periodic structures) or dots were formed on material surfaces using femtosecond laser processing.[13,14] Therefore, it is expected that the femtosecond laser processing is useful for surface modification of biomaterials.

Stem cell-based therapies have great potentials for the repair and regeneration of tissues or organs lost or damaged with any reasons such as accidents or diseases. Some of the co-authors of the present study have developed a novel tissue-engineering technique for tissue repair using a stem cell-based self-assembled tissue (scSAT) bio-synthesized from synovium-derived mesenchymal stem cells.[15] The scSAT consists of abundant type I and type III collagens, fibronectin and vitronectin, which are thought to be important constituents for tissue repair. Moreover, the scSAT is a scaffold-free construct composed of synovium-derived mesenchymal stem cells with their native extracellular matrices, it is free from concern regarding long-term immunological effects. Therefore, the scSAT is expected as a novel material for regenerative medicine, in particular for the repair of ligaments and tendons. However, the mechanical properties of the scSAT were insufficient for clinical application. Moreover, the structural and mechanical properties of the scSAT are isotropic while those of ligaments and tendons are anisotropic. To the problem, it may be a candidate of solutions to promote the generation of extracellular matrix in the scSAT by means of a special culture on a nano-structured surface. As described above, previous studies indicated that a material having a certain roughness promotes cell adhesiveness and that a material

having a periodic-pattern increases anisotropic property of cells.[10)]

Therefore, a nano-periodic patterned structure was processed on a titanium surface using a femtosecond laser system, and the adhesive and anisotropic properties of human synovium-derived mesenchymal stem cells to the processed surface were determined in the present study.

2. Materials and methods

2.1 Preparation of titanium specimens

Commercially available pure titanium disks with grade 2 (19 mmφ x 1.5 mm in thickness; Rare Metallic Co., Ltd., Tokyo, Japan) were wet-polished with SiC papers of grit number of 320, 600, 800, and 1,000 in the increasing order (Refinetec Co., Ltd., Kanagawa, Japan). Then, they were ultrasonically rinsed in acetone for 10 min and dried with air using an air pump. They were kept in an auto-dry desiccator. These titanium disks are named "Ti".

The nano-periodic structure on a Ti surface was patterned using a femtosecond laser apparatus (IFRIT, Cyber Laser Inc., Japan) with a seed laser (Femtolite, IMRA America Inc., Ann Arbor, MI, USA). The processing conditions were as follows: irradiation intensity of 700 mW, pulse repetition frequency of 1 kHz, pulse width of 190 fs, wavelength of 780 nm, beam diameter of 6 mm, focal distance of 60 mm, and scanning speed of 10 mm/s. The laser irradiation was defocused for 7 mm from the focal point. The titanium specimens subjected to nano-periodic processing are named "Nano-Ti".

2.2 Surface observation and characterization

The surfaces of Ti and Nano-Ti were observed using a scanning electron microscope (SEM: JSM-6380LA, JEOL Ltd., Tokyo, Japan) and an atomic force microscope (AFM: VN-8000, Keyence Co., Osaka, Japan). Scanning area of AFM observation was 2.5 μm x 2.5 μm. With the AFM observation, the surface characteristics such as pitch, ridge width, depth, and surface roughness were also determined using an analytical software equipped in the AFM. Three specimens (n=3) were prepared for each group, and measurement was performed at five different points in each specimen.

2.3 Isolation and cultivation of human synovium-derived mesenchymal stem cells

Human synovial membranes were obtained aseptically from the knee joints of patients during knee surgery on an agreement of tissue harvest. The method for the isolation and cultivation of human synovium-derived mesenchymal stem cells are described elsewhere.[15-17] Briefly, the synovial membrane specimens were rinsed with a phosphate buffered saline (PBS(-)) solution, minced meticulously, and digested with 0.1% type IV collagenase (Sigma-Aldrich Co., St. Louis, MO, USA) for 1.5 h at 37°C. After neutralization of the collagenase with growth medium containing high-glucose Dulbecco's modified Eagle's medium (Gibco BRL, Life Technologies Inc., Rockville, MD, USA) supplemented with 10% fetal bovine serum (FBS; Nichirei Biosciences Inc., Tokyo, Japan) and antibiotic (100 U/mL penicillin and 100 μg/mL streptomycin, Gibco BRL, Life Technologies Inc.), the cells were collected by centrifugation, washed with a PBS(-) solution, resuspended in growth medium, and plated in the tissue culture treated polystyrene dishes. The cells were cultured in the growth medium at 37°C in a humidified atmosphere of 5% CO_2. The medium was replaced once per week. After 14 d of primary cultivation, when the cells reached 80-100% confluence, they were washed twice with a PBS(-) solution, harvested by treatment with a trypsin-EDTA solution

(0.25% trypsin and 1 mM EDTA: Gibco BRL, Life Technologies Inc.), and replated at 1/5 dilutions for the first subculture. Cell passages were continued in the same manner with 1/5 dilutions when cultures reached near 100% confluence. The procedure of tissue harvest and subsequent cell culture were approved by the institutional review boards of Osaka University Medical School and Kogakuin University. Moreover, all procedures of this study followed the Declaration of Helsinki Principles.

Each titanium specimen was sterilized by autoclaving with reverse osmosis water and then placed on non-treated 12-well polystyrene dishes (22.1 mmφ). Then, the cells at 4-time passage were seeded on each specimen at a density of 3.0×10^3 cells/cm^2 and cultured for 1 h, 6 h, and 24 h.

2.4 Cellular attachment assays

For fluorescence microscopic observation, actin filaments, vinculin, and nuclei were stained. The cells were fixed with 4% paraformaldehyde solution. Nonspecific binding of the antibody was blocked by a blocking solution containing 5% goat serum in PBS(-) solution supplemented with 0.5% Tween20. The cells were reacted with monoclonal anti-vinculin (mouse IgG1 isotype) (Sigma-Aldrich Co.). Then, they were labeled with Alexa Fluor® 488-conjugated goat anti-mouse isotype-specific antibodies (Life Technologies Co., Carlsbad, CA, USA) and 0.7% rhodamine/phalloidin (Cytoskeleton Inc., Denver, CO, USA). Finally, nuclei were stained with 0.5% Hoechst33342 (Dojindo Laboratories Inc., Kumamoto, Japan). They were then observed using a fluorescence microscope (IX-7, Olympus Co., Tokyo, Japan).

For scanning electron microscopic (SEM) observation, the primary fixation of the cells on each specimen was performed by Karnovsky's fixative.[18] The secondary fixation was

performed using a 1% osmium tetraoxide solution. They were then gradually dehydrated in 50, 70, 80, 90, 95, and 100% ethanol, in increasing order, and dried in the CO_2 critical point drier. The cells on the specimens were then observed using a SEM (JSM-6380LA, JEOL Ltd.). The morphological parameters of the cells such as adhesion area, aspect ratio, and orientation angle were determined with ImageJ software (version 1.46, National Institutes of Health (NIH)). The outline of a cell in the SEM image was drawn and then the area of contoured part was calculated as cellular adhesion area. For the quantitative determinations of the aspect ratio and the orientation angle of the cell, the elliptical approximation of each cell was initially carried out on the SEM images.[19] The aspect ratio was calculated by dividing the elliptical long axis by its short axis. The orientation angle of the long axis of the cell with respect to the direction of the groove on Nano-Ti was calculated. The orientation angle on Ti was defined as the angle between the long axis of a cell and an arbitrary line. Ten cells on each specimen were analyzed to obtain average values for the adhesion area and aspect ratio. Fifty cells on each specimen were analyzed for the orientation angle.

2.5 Statistical analysis

All data were presented as mean ± standard deviation and were analyzed using the Student's two-tailed *t*-test with a significance level set at $P < 0.05$.

3. Results

3.1 Surface observation and characterization

Results of scanning electron microscopic observation are shown in Fig.1 while results of atomic force microscopic observation are shown in Fig.2. Region of interest for observation was randomly selected for each specimen. The surface geometry due to polish treatments with SiC papers was observed on Ti. On the other hand, the nano-sized periodic structure was observed on Nano-Ti surface. The orientation of the incident beam polarization was indicated in Fig.1d. The nano-periodic structure on the Nano-Ti exhibited 501 ± 100 nm of pitch, 99 ± 31 nm of depth, and 292 ± 50 nm of ridge. The parameters of surface roughness determined with AFM image data; the values of R_a, R_q, R_z, and R_v, were summarized in Table I. The roughness parameters of Nano-Ti were approximately 2-3 times higher than those of Ti.

3.2 Cell attachment, extension, and anisotropy

Results of fluorescence microscopic observation of cells cultured on Ti and Nano-Ti were shown in Figs.3, 4, and 5, respectively. Actin filament: a protein of cytoskeleton, vinculin: a membrane-cytoskeletal protein connecting integrin to actin cytoskeleton in focal adhesion plaques[20,21], and nucleus were indicated in a and e, b and f, and c and g, respectively. Composite images of actin filament, vinculin, and nucleus are shown in d and h. Note that the upper column (a, b, c, d) indicate cells on Ti while the lower column (e, f, g, h) indicate cells on Nano-Ti. The micrographs of cells cultured for 1 h and 6 h indicated that actin filaments and vinculin were more spread on Nano-Ti as compared with on Ti. It is, therefore, suggested that the cells on Nano-Ti exhibited more broad adhesion area than those on Ti at 1 h and 6 h of culture time (Figs.3 and 4). On the other hand, no significant differences in terms of the cell attachment and extension were observed at 24 h of culture time (Fig.5).

Scanning electron microscopic observation of cells cultured on Ti and Nano-Ti for 1 h, 6 h,

and 24 h were shown in Figs.6 and 7. The low magnification images showed that a cell cultured for 1 h on Nano-Ti was already extended (Fig.6d), though a cell shape on Ti was still spherical (Fig.6a). Moreover, the extension of a cell cultured for 6 h on Nano-Ti was greater than that on Ti (Figs.6b and 6e). In contrast, no significant difference in cell extension was observed between Ti and Nano-Ti at 24 h of culture time (Figs.6c and 6f). The high magnification images (Fig.7) showed that the fillopodia and lamellipodia of a cell had already extended on Nano-Ti at 1 h, though those on Ti had not been observed yet. Moreover, fillopodia and lamellipodia of the cell on Nano-Ti were extended more actively than those on Ti at 6 h. However, the fillopodia and lamellipodia of the cell on Ti were extended more actively than those on Nano-Ti at 24 h. Note that the fillopodia and lamellipodia of the cells on Nano-Ti were extended along the direction of grooves at 6 h and 24 h.

The adhesion areas of cells cultured for 1 h, 6 h, and 24 h are shown in Fig.8. The adhesion areas of cells cultured on Nano-Ti were significantly larger than those on Ti at 1 h and 6 h. However, no significant difference was observed in the areas of cells between Ti and Nano-Ti groups at 24 h. The aspect ratios of cells cultured for 1 h, 6 h, and 24 h are shown in Fig.9. The aspect ratio of cells on Nano-Ti was significantly higher than that on Ti at 6 h, though there were no significant difference in the aspect ratio between Ti and Nano-Ti groups at 1 h and 24 h. The orientation angles of cells cultured for 24 h are shown in Fig.10. Seventy eight percent of cells were distributed between −30° and 30°, and moreover, fifty percent of cells were distributed between −10° and 10° in Nano-Ti group. On the other hand, the orientation angles of cells were inconsistent in Ti group.

4. Discussion

Laser beam irradiation to a metallic substrate at an intensity around ablation threshold forms

nanoscopic levels of a periodic structure which is shaped like a grating. It has been reported that the threshold for forming a nano-periodic structure is approximately 0.1-1.0 J/cm^2.[22] In this study, a nano-periodic structure could not be patterned stably when the laser with the intensity of 0 mW was irradiated to a substrate at the focal point, because the laser intensity was fluctuated about 20 mW even if it was set at 0 mW. The diameter of condensing point is 15 μm when the laser was focused to the focal point. Therefore, the fluence of laser beam is 11.3 J/cm^2 when the laser intensity was 20 mW. This value of fluence was too strong to form a nano-periodic structure. Therefore, the laser was defocused for 7 mm from the focal point and the laser intensity was set at 700 mW. As a result, a nano-periodic structure was patterned stably. The fluence of laser beam became 0.203 J/cm^2 since the diameter of condensing point changes to 700 μm by defocusing. This value is in the range of threshold which allows to form a nano-periodic structure. In addition, the fluctuation of laser intensity at 700 mW with defocusing was smaller than those at 0 mW with focusing. Therefore, these laser irradiation conditions were suitable to pattern a nano-periodic structure stably on a titanium surface.

The formed pitch (501 ± 100 nm) was smaller than the wavelength of 780 nm of the nano-periodic structure. This result agreed well with a previous finding: the pitch (700 nm) was smaller than the wavelength (1,030 nm) in a femtosecond laser processing on titanium.[13] Similar tendency has been obtained on other substrates such as a copper, silicon wafer, and single crystals of MgF_2, BaF_2 and CaF_2.[14,22-24] However, the detailed mechanism of the tendency of laser processing has not been clarified. The surface roughness may be a factor which affects the processed pitches. In addition, the surface of pure titanium is stabilized by forming a thin oxide film of approximately 2-5 nm in thickness consisting of TiO_2, TiO, and Ti_2O_3.[25,26] The thin oxide film may affect the process of the nano-periodic structure. Further analyses and consideration as regard with factors affecting laser processing are

required.

In both the fluorescence microscopic and scanning electron microscopic observations (Figs.3, 4, 5, 6, and 7), the cells cultured on Nano-Ti extended over broader area than those on Ti at 1 h. The tendency similar to the cells cultured for 1 h was obtained in the cells cultured for 6 h. On the other hand, no significant difference was observed in terms of cell extension between the Ti and Nano-Ti groups at 24 h. The cells exhibited spherical shape at first, and then, they extended gradually after contacting on a material surface, and finally, they became spindle-shape. In general, cell adhesion and extension are completed sufficiently within 24 h, as shown in Fig.8. Although the cells were round-shape in both the Ti and Nano-Ti groups at 1 h of culture, they gradually became spindle-shape in the Nano-Ti group while they remained unchanged in the Ti group at 6 h of culture. Finally, the cells became spindle-shape in both the groups at 24 h of culture as shown in Fig.9. Therefore, it was indicated that Nano-Ti promoted the process of cell adhesion and extension. When the cells attach to and extend on the substrate, they spread their fillopodia and lamellipodia.[27] The extension occurred earlier around 1 h, continued around 6 h, and almost completed by 24 h in the Nano-Ti group as found in Fig.8. However, the extension occurred around 6 h, and still continued at 24 h in the Ti group. These results also suggest that Nano-Ti promoted the process of cell extension.

Fig.10 showed that the approximately 80% of cells on Nano-Ti were distributed within ± 30° with respect to the direction of nano-patterned grooves. Moreover, fillopodia and lamellipodia of cells on Nano-Ti spread along grooves. These results clearly indicated that Nano-Ti promoted the process of cell orientation. Results of the AFM observation and analysis indicated that the pitch, ridge width, and depth of Nano-Ti were 501 ± 100 nm, 292 ± 50 nm, and 99 ± 31 nm, respectively. It has been reported that the fibroblast alignment was promoted on groove ridge width larger than 100 nm.[28] In addition, it has been reported that

mesenchymal stem cells could recognize the grooves that were deeper than 90 nm.[29] Nano-Ti surface processed in this study fulfills all of these parameters. Therefore, Nano-Ti patterned in this study was suitable for cell adhesion, extension, and orientation.

5. Conclusions

In the present study, morphological observations were performed on human synovium-derived mesenchymal stem cells cultured on a nano-periodic patterned titanium structure processed using a femtosecond laser system. Results reveal that the patterned structure promotes the adhesive and anisotropic properties of the cells. It is suggested that the femtosecond laser processing technique is useful for the development and modification of cell-based biomaterials.

Acknowledgements

The present study was financially supported in part by the MEXT-Supported Program for the Strategic Research Foundation at Private Universities, 2008-2012 (BERC, Kogakuin University).

References

1) J. Y. Martin, Z. Schwartz, T. W. Hummert, D. M. Schraub, J. Simpson, J. Lankford Jr, D. D. Dean, D. L. Cochran, and B. D. Boyan: J. Biomed. Mater. Res. **29** (1995) 389.

2) K. Kieswetter, Z. Schwartz, T. W. Hummert, D. L. Cochran, J. Simpson, D. D. Dean, and B. D. Boyan: J. Biomed. Mater. Res. **32** (1996) 55.

3) B. D. Boyan, R. Batzer, K. Kieswetter, Y. Liu, D. L. Cochran, S. Szmuckler-Moncler, D. D. Dean, and Z. Schwartz: J. Biomed. Mater. Res. **39** (1998) 77.

4) L. Zhang, V. M. Menendez-Flores, N. Murakami, and T. Ohno: Appl. Surf. Sci. **258** (2012) 5803.

5) S. Ban, Y. Iwaya, H. Kono, and H. Sato: Dent. Mater. **22** (2006) 1115.

6) H. Asoh, K. Uchibori, and S. Ono: Semicond. Sci. Tech. **26** (2011) 102001.

7) H. Asoh, F. Arai, and S. Ono: Electrochim. Acta **54** (2009) 5142.

8) D. Z. Xie, B. K. A. Ngoi, Y. Q. Fu, A. S. Ong, and B. H. Lim: Appl. Serf. Sci. **225** (2004) 54.

9) S. Rennon, L. Bach, H. König, J. P. Reithmaier, A. Forchel, J. L. Gentner, and L. Goldstein: Microelectron. Eng. **57-58** (2001) 891.

10) A. I. Teixeira, G. A. Abrams, P. J. Bertices, C. J. Murphy, and P. F. Nealey: J. Cell Sci. **116** (2003) 1881.

11) Y. B. Xiao, E. H. Kim, S. M. Kong, J. H. Park, B. C. Min, and C. W. Chung: Vacuum **85** (2010) 434.

12) K-H. Leitz, B. Redlingshöfer, Y. Reg, A. Otto, and M. Schmidt: Phys. Procedia **12** (2011) 230.

13) V. Oliveira, S. Ausset, and R. Vilar: Appl. Surf. Sci **255** (2009) 7556.

14) J. Reif, O. Varlamova, and F. Costache: J. Appl. Phys. **92** (2008) 1019.

15) W. Ando, K. Tateishi, D. A. Hart, D. Katakai, Y. Tanaka, K. Nakata, J. Hashimoto, H. Fujie, K. Shino, H. Yoshikawa, and N. Nakamura: Biomaterials **28** (2007) 5462.

16) W. Ando, K. Tateishi, D. Katakai, D. A. Hart, C. Higuchi, K. Nakata, J. Hashimoto, H. Fujie, K. Shino, H. Yoshikawa, and N. Nakamura: Tissue Eng. Part A **14** (2008) 2014.

17) K. Shimomura, W. Ando, K. Tateishi, R. Nansai, H. Fujie, D. A. Hart, H. Kohda, K. Kita, T. Kanamoto, T. Mae, K. Nakata, K. Shino, H. Yoshikawa, N. Nakamura: Biomaterials **31** (2010) 8004.

18) M. J. Karnovsky: J. Cell Biol. **27** (1965) 137A.

19) S. Fujita, M. Ohshima, and H. Iwata: J. R. Soc. Interface **6** (2009) S269.

20) D. R. Critchley: Biochem. Soc. Trans. **32** (2004) 831.

21) V. E. Koteliansky, E. P. Ogryzko, N. I. Zhidkova, P. A. Weller, D. R. Critchley, K. Vancompernolle, J. Vandekerckhove, P. Strasser, M. Way, M. Gimona, and J. V. Small: Biochem. Eur. J. Biochem. **204** (1992) 767.

22) S. Sakabe, M. Hashida, S. Tokita, S. Namba, and K. Okamuro: Phys. Rev. B **79** (2009) 033409.

23) F. Costache, M. Henyk, J. Reif: Appl. Surf. Sci. **208-209** (2003) 486-491.

24) D. V. Tran, H. Y. Zheng, Y. C. Lam, V. M. Murukeshan, J. C. Chai, and D. E. Hardt: Opt. Lasers Eng. **43** (2005) 977.

25) K. Oya, Y. Tanaka, Y. Moriyama, Y. Yoshioka, T. Kimura, Y. Tsutsumi, H. Doi, N. Nomura, K. Noda, A. Kishida, and T. Hanawa: J. Biomed Mater. Res. A **94** (2010) 611.

26) Y. Tsutsumi, D. Nishimura, H. Doi, N. Nomura, and T. Hanawa: Mater. Sci. Eng. C **29** (2009) 1702.

27) B. Alberts, A. Johnson, J. Lewis, M. Raff, K. Roberts, and P. Walter: *Mol. Biol. Cell* (Garland Science, Abingdon, UK, 2008) 5th ed., p.996, 1006, 1037, 1040, and 1041.

28) W. A. Loesberg, J. te Riet, F. C. M. J. M. van Delft, P. Schon, C. G. Figdor, S. Speller, J.

J. W. A. van Loon, X. F. Walboomers, and J. A. Jansen: Biomaterials **28** (2007) 3944.

29) S. Fujita, D. Ono, M. Ohshima, H. Iwata: Biomaterials **29** (2008) 4494.